Original Article

MOLECULAR METABOLISM

High-fat diet induces time-dependent synaptic plasticity of the lateral hypothalamus

Victoria Linehan [1], **Lisa Z. Fang** [1], **Matthew P. Parsons**, **Michiru Hirasawa***

ABSTRACT

Objective: Orexin (ORX) and melanin-concentrating hormone (MCH) neurons in the lateral hypothalamus are critical regulators of energy homeostasis and are thought to differentially contribute to diet-induced obesity. However, it is unclear whether the synaptic properties of these cells are altered by obesogenic diets over time.

Methods: Rats and mice were fed a control chow or palatable high-fat diet (HFD) for various durations and then synaptic properties of ORX and MCH neurons were examined using *ex vivo* whole-cell patch clamp recording. Confocal imaging was performed to assess the number of excitatory synaptic contacts to these neurons.

Results: ORX neurons exhibited a transient increase in spontaneous excitatory transmission as early as 1 day up to 1 week of HFD, which returned to control levels with prolonged feeding. Conversely, HFD induced a delayed increase in excitatory synaptic transmission to MCH neurons, which progressively increased as HFD became chronic. This increase occurred before the onset of significant weight gain. These synaptic changes appeared to be due to altered postsynaptic sensitivity or the number of active synaptic contacts depending on cell type and feeding duration. However, HFD induced no change in inhibitory transmission in either cell type at any time point.

Conclusions: These results suggest that the effects of HFD on feeding-related neurons are cell type-specific and dynamic. This highlights the importance of considering the feeding duration for research and weight loss interventions. ORX neurons may contribute to early hyperphagia, whereas MCH neurons may play a role in the onset and long-term maintenance of diet-induced obesity.

Keywords Orexin; Melanin-concentrating hormone; Synaptic transmission; High-fat diet; Diet-induced obesity

1. INTRODUCTION

The global incidence of obesity is increasing, leading to a concomitant rise in its associated comorbidities, including type II diabetes, cardiovascular disease, and some cancers. Most prevalent is diet-induced obesity (DIO), which is typically caused by an overconsumption of energy-dense foods without a sufficient increase in energy expenditure to compensate.

DIO is associated with functional and structural changes in the hypothalamic neuronal circuitry controlling energy balance. For instance, synaptic remodeling occurs within the arcuate nucleus of rodent models of DIO, characterized by a change in the number of excitatory and inhibitory synaptic contacts to neuropeptide Y and proopiomelanocortin neurons [1,2]. These changes are thought to be a homeostatic negative feedback mechanism underlying counter-regulatory responses to elevated caloric intake and fat mass. However, high-fat diet (HFD), commonly used in DIO models, can drive caloric overconsumption through a positive feedback mechanism involving the reward system [3]. These functionally opposing negative and positive feedback mechanisms are likely to be dynamically regulated during the development and maintenance phases of DIO.

The hypothalamic energy balance circuitry is comprised of several nuclei, including the arcuate nucleus, lateral hypothalamus (LH), ventromedial hypothalamus, and paraventricular nucleus [4]. Moreover, the LH is uniquely connected to the reward system to mediate the motivation to work for food and other rewards [5]. Within the LH, orexin (ORX) and melanin-concentrating hormone (MCH) neurons are two distinct peptidergic cell types that underlie these functions. These cell populations are known for their complementary and partially antagonistic roles in energy balance and reward [6] through reciprocal connections to related brain regions [7–10].

Both ORX and MCH neurons are orexigenic, as acute application of these neuropeptides induces food intake [11,12]. Yet, ORX-induced food intake and weight gain diminishes with prolonged infusion [13],

Division of Biomedical Sciences, Faculty of Medicine, Memorial University, 300 Prince Philip Drive, St. John's, Newfoundland, A1B 3V6, Canada

[1] Victoria Linehan and Lisa Z. Fang contributed equally to this work.

*Corresponding author. Division of Biomedical Sciences, Faculty of Medicine, Memorial University, 300 Prince Philip Drive, St. John's, NL, A1B 3V6, Canada. Tel.: +1 709 864 6573. E-mail: michiru@mun.ca (M. Hirasawa).

Abbreviations: ACSF, artificial cerebrospinal fluid; CV, coefficient of variation; D-AP5, D-(−)-2-Amino-5-phosphonopentanoic acid; DIO, diet-induced obesity; DNQX, 6,7-Dinitroquinoxaline-2,3-dione; EPSC, excitatory postsynaptic current; eEPSC, evoked excitatory postsynaptic current; HFD, high-fat diet; IPSC, inhibitory postsynaptic current; LH, lateral hypothalamus; MCH, melanin-concentrating hormone; mEPSC, miniature excitatory postsynaptic current; mIPSC, miniature inhibitory postsynaptic current; NSNA, non-stationary noise analysis; ORX, orexin; PPR, paired pulse ratio

Received September 18, 2019 • Revision received February 28, 2020 • Accepted March 10, 2020 • Available online 18 March 2020

https://doi.org/10.1016/j.molmet.2020.100977

whereas chronic administration of MCH induces sustained hyperphagia and obesity [14,15], suggesting differential roles in long-term energy balance. ORX neurons are activated by HFD [16], food-associated cues [17–19], and other highly salient stimuli [20,21]. Furthermore, postnatal ablation of ORX neurons leads to reduced food intake [22], while their ablation in adulthood results in a modest increase in food intake [7], suggesting that age may be a factor in energy balance mechanisms. ORX signaling also promotes arousal and motivation to seek and consume palatable food [19], while increasing metabolism, sympathetic activation, and locomotor activity [23,24]. In sum, despite promoting acute food intake, the net result of ORX signaling is negative energy balance and resistance to DIO [25]. Thus, previous studies overall indicate that ORX neurons play an integrated role in goal-directed behaviors where motivational activation is matched by arousal and physical activity. In contrast, MCH neurons promote a positive energy balance and higher body weight. Activation of these neurons promotes the preference and consumption of food according to its nutrient value [26]. MCH stimulates food intake, particularly palatable,calorie-dense food [15,27], while promoting energy conservation through reduced metabolism and locomotor activity [28,29]. Together, these studies delineate the complementary roles of ORX and MCH in different aspects of food intake control and opposing effects on overall energy balance.

The activity of ORX and MCH neurons is regulated by excitatory and inhibitory synaptic inputs whose functional properties change during development in a cell-type specific manner. While excitatory synapses to ORX neurons functionally mature before adolescence (prior to weaning), MCH neurons take much longer to reach the adult level [30]. How these age-dependent synaptic properties interact with prolonged HFD exposure remains obscure. Therefore, the present study investigates the synaptic effects of HFD on ORX and MCH neurons in rats from adolescence to adulthood. This study provides novel insights into the impact of HFD on the regulatory mechanisms involved in energy homeostasis. This has important implications in present society, given the abundance of palatable energy-dense foods that are widely available starting from a very young age.

2. METHODS

2.1. Animals

All of the experiments were conducted following the guidelines of the Canadian Council of Animal Care and were approved by Memorial University's Institutional Animal Care Committee. Male Sprague–Dawley rats (Charles River, Saint Constant, Canada or Memorial University breeding colony) and C57BL/6NCrl (Charles River, Saint Constant, Canada) were fed *ad libitum* with a standard chow (LabDiet autoclavable rodent diet 5010, 12.7% fat) or a palatable HFD (TestDiet AIN-76A Western Diet, 40.1% fat). Body weight and food intake were measured weekly. Animals were 3 weeks old at the start of the feeding period unless stated otherwise. For 1-day HFD, the feeding period was staggered so that the rats were 4 weeks old at the time of electrophysiological recordings.

2.2. Electrophysiology

Following the feeding period, rats and mice were deeply anesthetized with isoflurane and the brain was removed. Acute 250-μm slices of the hypothalamus were generated using a vibratome (VT-1000, Leica Microsystems) in cold artificial cerebrospinal fluid (ASCF; composition: (in mM): 126 NaCl, 2.5 KCl, 1.2 NaH_2PO_4, 1.2 $MgCl_2$, 2 $CaCl_2$, 18 $NaHCO_3$, and 2.5 glucose) and bubbled with 95% O_2/5% CO_2. Slices were incubated at 32–34 °C for 30 min and then maintained at room temperature until the experiments were conducted. For whole-cell patch clamp recordings, hemisected slices were placed in a recording chamber perfused with ACSF at 1–2 mL/min, 32 °C. Glass pipette recording electrodes had a tip resistance of 3–5 MΩ when filled with internal solution (for EPSCs (in mM): 123 K-gluconate, 2 $MgCl_2$, 8 KCl, 0.2 EGTA, 10 HEPES, 5 Na_2-ATP, 0.3 Na-GTP, and 2.7 biocytin; for IPSCs, K-gluconate was replaced with equimolar KCl). Whole-cell series/access resistance was 5–20 MΩ, which was monitored throughout the recording by applying a 20-mV, 50-ms square pulse every minute. MultiClamp 700B and pClamp 9 or 10 software (Molecular Devices, Sunnyvale, CA, USA) were used to collect the data. Signals were filtered at 1 kHz and digitized at 5–10 kHz.

All voltage clamp recordings were performed at a holding potential of −70 mV. Picrotoxin (50 μM; Sigma, Oakville, Canada) was applied in the bath to isolate the excitatory postsynaptic current (EPSC), while 6,7-dinitroquinoxaline-2,3-dione (DNQX 10 μM; Tocris Bioscience, Minneapolis, MN, USA) and D-2-amino-5-phosphonopentanoic acid (D-AP5 50 μM; Abcam, Cambridge, MA, USA) were used to record the inhibitory postsynaptic current (IPSC). In addition, action potential-independent miniature EPSC or IPSC (mEPSC and mIPSC, respectively) were isolated using tetrodotoxin (1 μM; Alomone Labs, Jerusalem, Israel).

To assess evoked EPSC (eEPSC) amplitude and paired pulse ratio (PPR), a pair of eEPSCs at 50 Hz was elicited every 15 s via a glass stimulating electrode filled with ACSF, which was placed medially to the recorded cell. The stimulus intensity required to elicit approximately 50% of the maximal eEPSC amplitude for each recorded cell was used. PPR was calculated as the eEPSC2/eEPSC1.

2.3. Identification of ORX and MCH neurons

ORX and MCH neurons can be distinguished with high accuracy among other neurons in the LH based on a unique set of electrophysiological responses to negative and positive current injections (600 ms, incremental steps from −200 to +200 pA) [31,32]. Briefly, ORX neurons display an H current and a rebound depolarization following relief from hyperpolarization, which is capped by action potentials in some cells. They also fire spontaneously and display a uniphasic afterhyperpolarizing potential. MCH neurons are typically not spontaneously active, but upon positive current injections, display action potentials with uniphasic afterhyperpolarizing potential and spike adaptation. These cells also show no H current and no rebound during or following hyperpolarization, respectively.

Post-hoc immunohistochemistry was performed on a subset of cells labeled with biocytin during patch clamp recording. Following experiments, brain slices were fixed in 10% formalin for at least 12 h. Subsequently, the slices were incubated with goat anti-ORX-A IgG (1:2000; SC8070, Santa Cruz Biotechnology, Dallas, TX, USA) and rabbit anti-MCH IgG (1:1000–2000; H-070-47, Phoenix Pharmaceuticals, Burlingame, CA, USA) for 3 days at 4 °C. Then appropriate secondary antibodies and Alexa 350-conjugated streptavidin (1:500; Jackson ImmunoResearch, West Grove, PA, USA) were applied for 3 h at room temperature or overnight at 4 °C. Colocalization of biocytin with either ORX-A or MCH was assessed using an epifluorescence microscope.

Electrophysiologically identified putative ORX or MCH neurons were confirmed immunopositive for the respective peptide in 177 of 178 rat ORX neurons and 143 of 144 rat MCH neurons tested (success rate 99.4%), 31 of 31 mouse ORX neurons, and 22 of 22 mouse MCH neurons tested (success rate 100%). The remaining cells immunonegative for ORX and MCH were removed from further analysis. A total of 276 ORX neurons and 205 MCH neurons from 113 rats and 39 ORX

neurons and 32 MCH neurons from 30 mice that displayed the characteristic electrophysiological fingerprints were included in the study.

2.4. Double immunohistochemistry

Three-week-old rats were fed for 4 weeks with chow (4wCtrl) or HFD (4wHFD), and six-week-old rats were fed HFD for 1 week (1wHFD). After the feeding period, rats were deeply anesthetized with isoflurane and transcardially perfused with 4% paraformaldehyde (PFA). Their brains were removed, post-fixed overnight in 4% PFA, and serially cryoprotected in 15% then 30% sucrose in PBS. Then 16-μm sections containing the hypothalamus were collected using a cryostat (CM 3050S, Leica Microsystems). For immunofluorescence, the tissue sections were incubated overnight at 4 °C in guinea pig anti-vGluT2 IgG (1:500; 135 404, Synaptic Systems, Goettingen, Germany) and either goat anti-proMCH IgG (1:500; sc14509, Santa Cruz Biotechnology, Dallas, TX, USA) or goat anti-ORX-A IgG (1:500; sc8070, Santa Cruz Biotechnology, Dallas, TX, USA). The next day, the sections were incubated in Cy3-conjugated anti-guinea pig IgG (1:500; 706-165-148, Jackson ImmunoResearch, West Grove, PA, USA) and AlexaFluor 488-conjugated anti-goat IgG (1:500; A11055, Invitrogen) for 2 h at room temperature. The slides were coverslipped using Dako fluorescence mounting medium (Agilent Technologies, Inc., Santa Clara, CA, USA) and stored at 4 °C until imaging.

2.5. Confocal imaging and analysis

Neurons immunopositive for ORX-A or MCH with clear nuclei were randomly selected for imaging within the LH dorsal to the fornix. Next, 5-μm z-stacks (5 sections at 1 μm intervals) were taken at 60X (1.42 NA) magnification using a laser-scanning confocal microscope (Fluoview FV1000, Olympus Corporation) and Z-projected images were generated. The following steps were performed using ImageJ by experimenters blind to the experimental groups. First, a pilot study was conducted to determine an appropriate threshold for positive vGluT2 by testing a series of thresholds on a random set of vGluT2-stained sections, followed by visual comparison of the resulting binary images to the original. Next, a threshold was applied separately to grayscale images of neuropeptides or vGluT2 to generate binary images. The threshold for vGluT2 was set at 10% of the pixel intensity distribution based on the pilot study. The binary images were merged and the number of vGluT2 puncta directly apposed to the MCH or ORX neuron somata were counted.

2.6. Data analysis

MiniAnalysis software (Synaptosoft, Inc.) was used to measure the frequency and amplitude of the mEPSCs and mIPSCs and perform peak scaled non-stationary noise analysis (NSNA) from 3 min of consecutive voltage clamp traces recorded from each cell. The relative distribution of the mEPSC amplitude in each cell was fit with a Gaussian regression to determine the peak of the mEPSC amplitude distribution. The coefficient of variation (CV) was calculated as the product of the standard deviation divided by the mean. The evoked EPSC amplitude was analyzed using Clampfit 10 and the PPR was calculated as EPSC2/EPSC1.

Data are expressed as mean ± SEM. The number of cells (n) and animals (N) used are indicated in the corresponding figure legend. Unpaired t-tests and one-way and two-way ANOVA were performed using Prism 7 (GraphPad Software) to assess statistical differences between groups and test the effect of diet. If ANOVA indicated significance, a Sidak multiple comparisons test was performed. $P < 0.05$ was considered significant.

3. RESULTS

Three-week-old rats that were fed HFD for 11 weeks gained substantially more weight than their control chow (Ctrl)-fed counterparts (Figures. S1A and C). While the difference in body weight did not become significant until 5 weeks of feeding, the HFD-fed rats consumed significantly more calories throughout the duration of feeding (Figure S1B). At the end of the feeding period, the HFD group had significantly heavier white adipose tissues (epididymal and retroperitoneal fat pads) than the Ctrl group (Figures. S1D and E). Based on these observations, we selected 3 time points for electrophysiological analysis: an acute phase (1-week feeding), a phase prior to the onset of significant differences in body weight (4-week feeding), and a chronic phase where body weight and caloric intake was persistently higher in the HFD group (11- to 14-week feeding; referred to as 11-week feeding for simplicity for the remainder of the results).

3.1. Orexin neurons

In ORX neurons, 1 week of HFD feeding induced an increase in mEPSC amplitude (Figure 1A,C). This was accompanied by a rightward shift in the peak of amplitude distribution (Figure 1B,D). HFD also had a main effect on the CV but without significant changes at each time point (Figure 1E). This suggests a general increase in the amplitude of mEPSCs, as opposed to an increase in the proportion of larger events skewing the distribution. Similar effects were already present after 1 day of HFD (1dHFD; Figure 1B [top panel] and Figure S2A). However, these changes were transient, as the mean mEPSC amplitude and peak of frequency distribution returned to Ctrl levels by 4 and 11 weeks of feeding (Figure 1C—D).

To determine the mechanism underlying the increase in mEPSC amplitude, a peak-scaled NSNA was conducted to estimate the number and conductance of postsynaptic AMPA receptors [33] (Figure 1F,G and Figure S3). Interestingly, Ctrl ORX neurons displayed an age-dependent increase in estimated single channel currents (Figure 1F) and a reduction in estimated number of channels (Figure 1G). After 1 week of HFD, a marked increase in the estimated single channel current was observed without a change in the estimated receptor numbers relative to the Ctrl (Figure 1F—G). Similar changes were already observed after 1 day of HFD (Figures S2B—C and Figure S3B [left panel]), but returned to Ctrl levels after 4 or 11 weeks of feeding (Figure 1F—G). These results suggest that the transient, early increase in mEPSC amplitude in ORX neurons was likely due to an increase in AMPA receptor conductance.

Analysis of mEPSC frequency revealed a different time course of the HFD effect. In contrast to the early change in mEPSC amplitude, mEPSC frequency was not affected by 1 week of HFD but was significantly increased by 4 weeks before returning to Ctrl levels after 11 weeks (Figure 2A—B). If this were due to an increase in release probability, the eEPSC amplitude would be expected to increase and the PPR to decrease. However, there was no difference in the eEPSC amplitude (50% max) (Figure 2C—D). In addition, there was a main effect of HFD to slightly increase PPR through the feeding period but without significant post-hoc differences at each time point (Figure 2E). These results together led us to hypothesize that 4 weeks of HFD induced a transient increase in the number of excitatory synaptic contacts to ORX neurons rather than increasing the presynaptic release probability.

To test this hypothesis, a confocal analysis was performed to assess the number of excitatory terminals in contact with ORX neurons. To eliminate any possible changes in synaptic connections due to development, age-matched animals were used for this comparison. Specifically, 6-week-

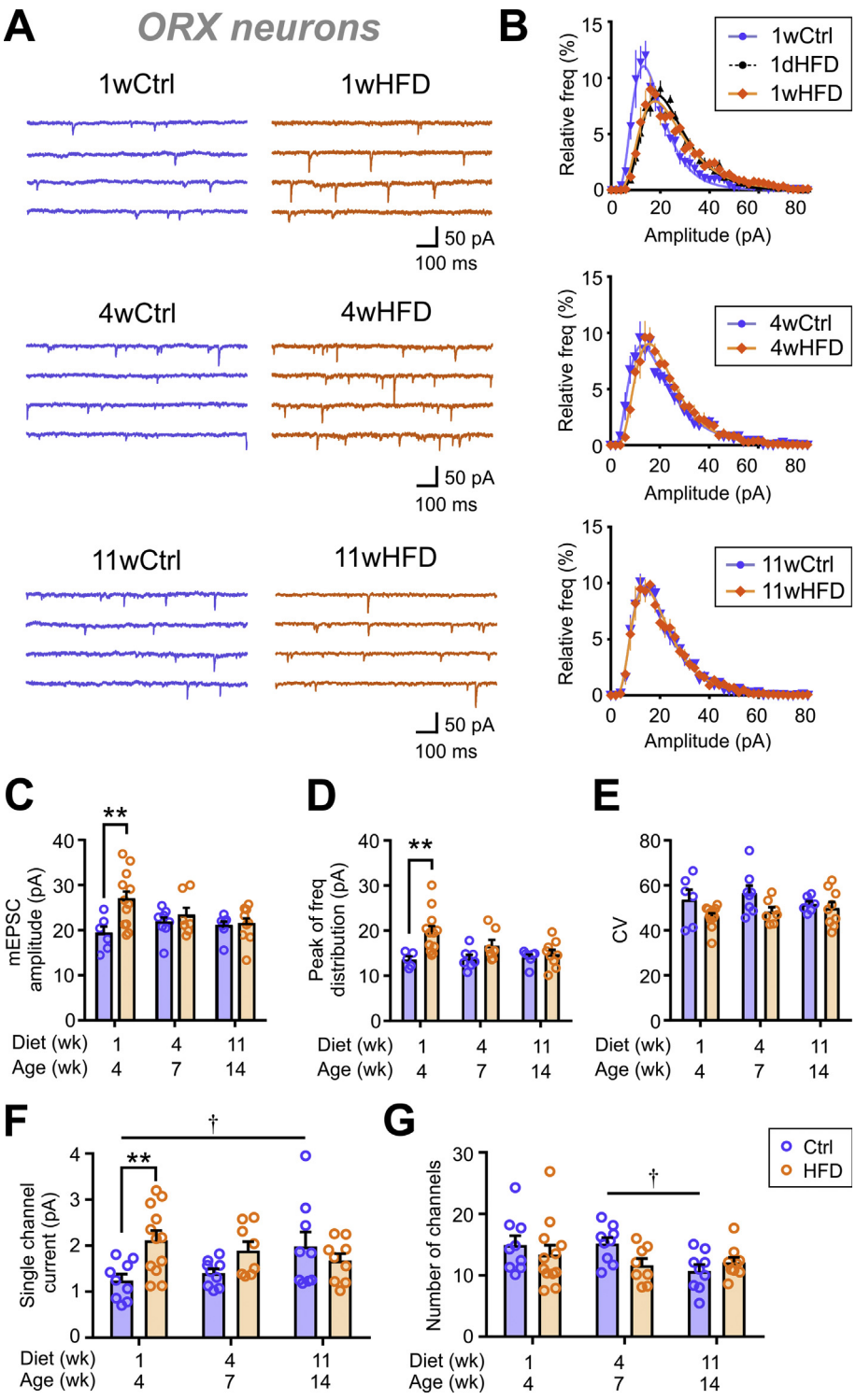

Figure 1: HFD transiently increases mEPSC amplitude in ORX neurons. (A) Representative mEPSC traces from ORX neurons of rats fed a control chow (Ctrl; left) or high-fat diet (HFD; right) for 1 week (1w), 4 weeks (4w), and 11 weeks (11w). (B) Relative frequency distribution of mEPSC amplitudes of ORX neurons. Plots represent averages of the Ctrl or HFD groups with different feeding durations as indicated. (C–D) Summary graphs displaying an early transient increase in mEPSC amplitude (C; two-way ANOVA, $p = 0.0185$) and the peak of relative frequency distributions shown in B (D; two-way ANOVA, $p = 0.0010$). (E) HFD has an overall effect on the coefficient of variation (CV) of mEPSC amplitude (two-way ANOVA, $p = 0.0085$) but without post-hoc significance at each time point. (F) Summary graph showing an HFD-induced early transient increase in the estimated single channel current (two-way ANOVA, $p = 0.0378$). There is also an age-dependent change among the Ctrl groups (one-way ANOVA, $p = 0.0390$). (G) Summary graph showing the estimated number of channels. There is no effect of HFD (two-way ANOVA, $p = 0.4464$); however, the Ctrl group displayed a decrease in the estimated number of channels with age (one-way ANOVA, $p = 0.0277$). See Figure S3 for representative recordings and non-stationary noise analysis (NSNA) of mEPSCs. $^{**}p < 0.01$ for Ctrl vs HFD, $\dagger p < 0.05$ for age, Sidak's multiple comparison test. $n = 6–12$ cells; $N = 4–7$ rats.

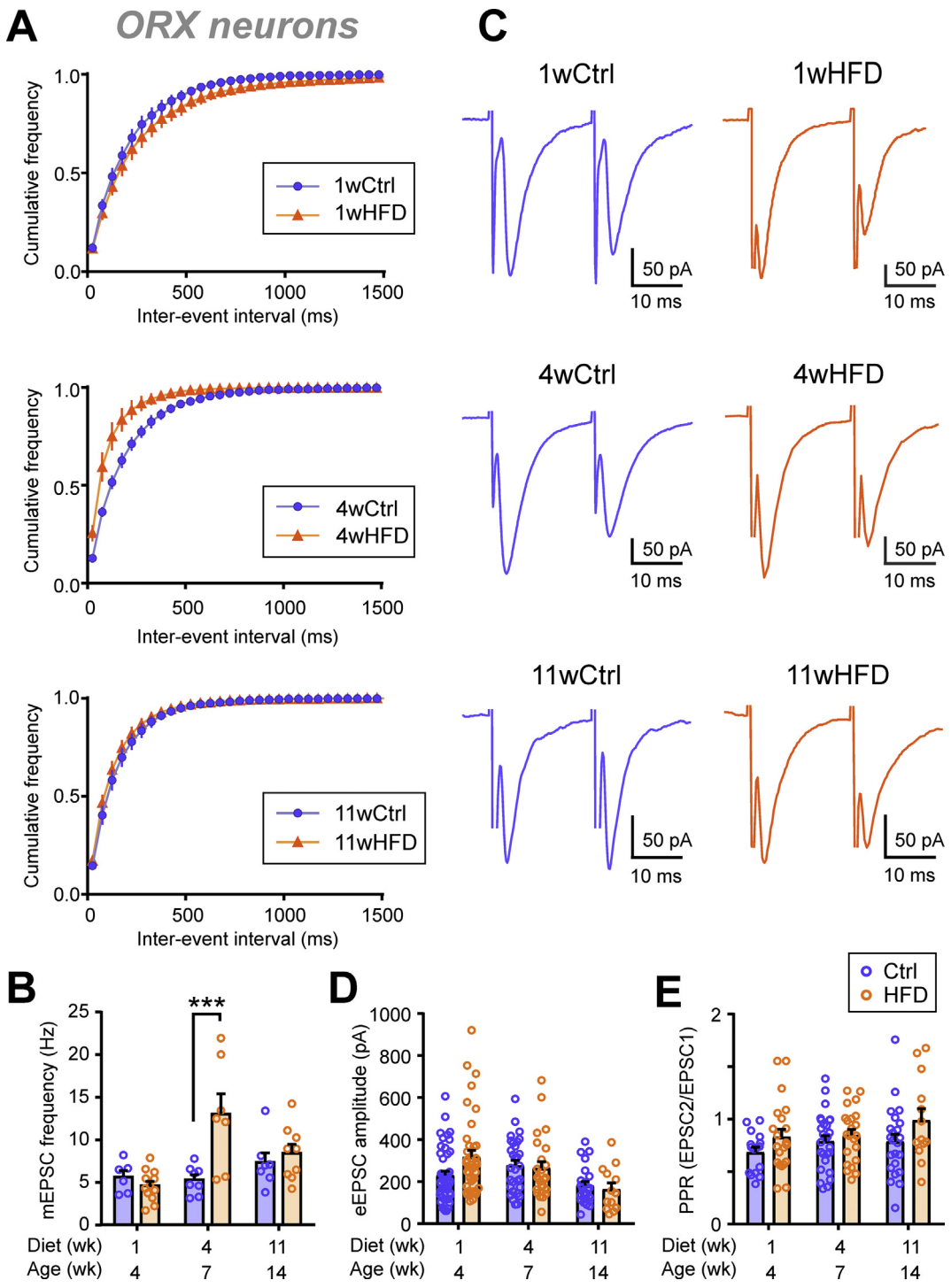

Figure 2: HFD transiently increases mEPSC frequency without changes in paired pulse ratio. (A) Averaged cumulative frequency distribution of mEPSC inter-event interval of ORX neurons. (B) HFD induces a delayed, transient increase in the mEPSC frequency after 4 weeks of feeding (two-way ANOVA, $p = 0.0090$). (C) Representative paired EPSCs from ORX neurons in the Ctrl (left) and HFD (right) groups with different feeding durations as indicated. (D) HFD has no effect on the evoked EPSC (eEPSC) amplitude (two-way ANOVA, $p = 0.4145$). (E) HFD has a main effect on PPR (two-way ANOVA, $p = 0.0167$) but without significant post-hoc differences at each time point. ***$p < 0.001$ for Ctrl vs HFD, Sidak's multiple comparison test. $n = 13–45$ cells; $N = 4–29$ rats.

old rats were fed HFD for 1 week, and 3-week-old rats were fed chow or HFD for 4 weeks, such that all rats were 7 weeks of age at the end of the feeding period. In these age-matched rats, 1 week of HFD induced an increase in mEPSC amplitude but no change in mEPSC frequency (Figure 3A–B), which was similar to the results from the adolescence period. However, there was no change in the number of vGluT2 puncta in apposition with ORX neurons at 1 or 4 weeks (Figure 3C–F). Together, these results suggest that increased mEPSC frequency after 4

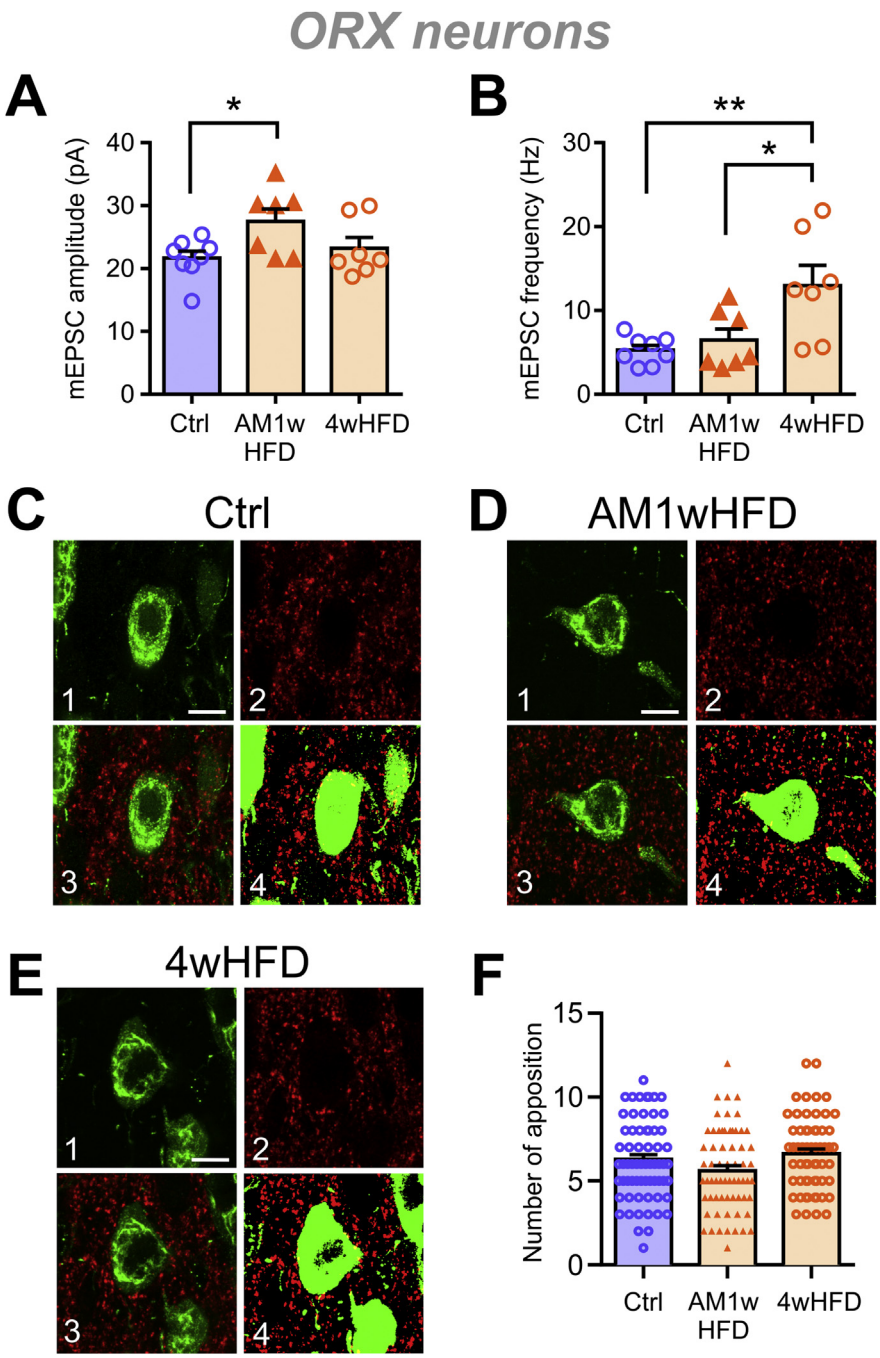

Figure 3: HFD does not influence the number of excitatory synapses to ORX neuron somata. Feeding periods were staggered so that all rats were 7 weeks old at the time of assessment. (A–B) ORX neurons from the age-matched 1-week HFD group (AM1wHFD) show a larger mEPSC amplitude (A) but no change in the mEPSC frequency compared to Ctrl (B). By 4 weeks (4wHFD), there was a significant increase in the mEPSC frequency. One-way ANOVA: mEPSC amplitude (A), $p = 0.0255$; mEPSC frequency (B), $p = 0.0058$. *$p < 0.05$, **$p < 0.01$, Sidak's multiple comparison test. $n = 7–10$ cells, $N = 4–7$ rats. (C–E) Representative immunofluorescence images of the lateral hypothalamus. Panels show confocal images of ORX-A+ neurons (green; C1, D1, and E1), vGluT2+ glutamatergic puncta (red; C2, D2, and E2), the merged confocal image containing both channels (C3, D3, and E3), and the merged binary image used for analysis generated by applying a threshold to individual channels (C4, D4, and E4). Scale bar = 10 μm. (F) No difference in the number of vGluT2+ appositions to ORX neuron somata is found among the feeding groups (one-way ANOVA, $p = 0.0526$). For (C–F): $n = 59–65$ neurons from 2-4 slices per rat, $N = 3–4$ rats per diet condition.

weeks of HFD may not involve synaptic remodeling at ORX neuron somata, although possible remodeling at the dendrites cannot be excluded.

Next, inhibitory transmission to ORX neurons was investigated. Notably, Ctrl ORX neurons showed an age-dependent decline in mIPSC amplitude (Figure 4A–B), while the frequency remained stable (Figure 4C).

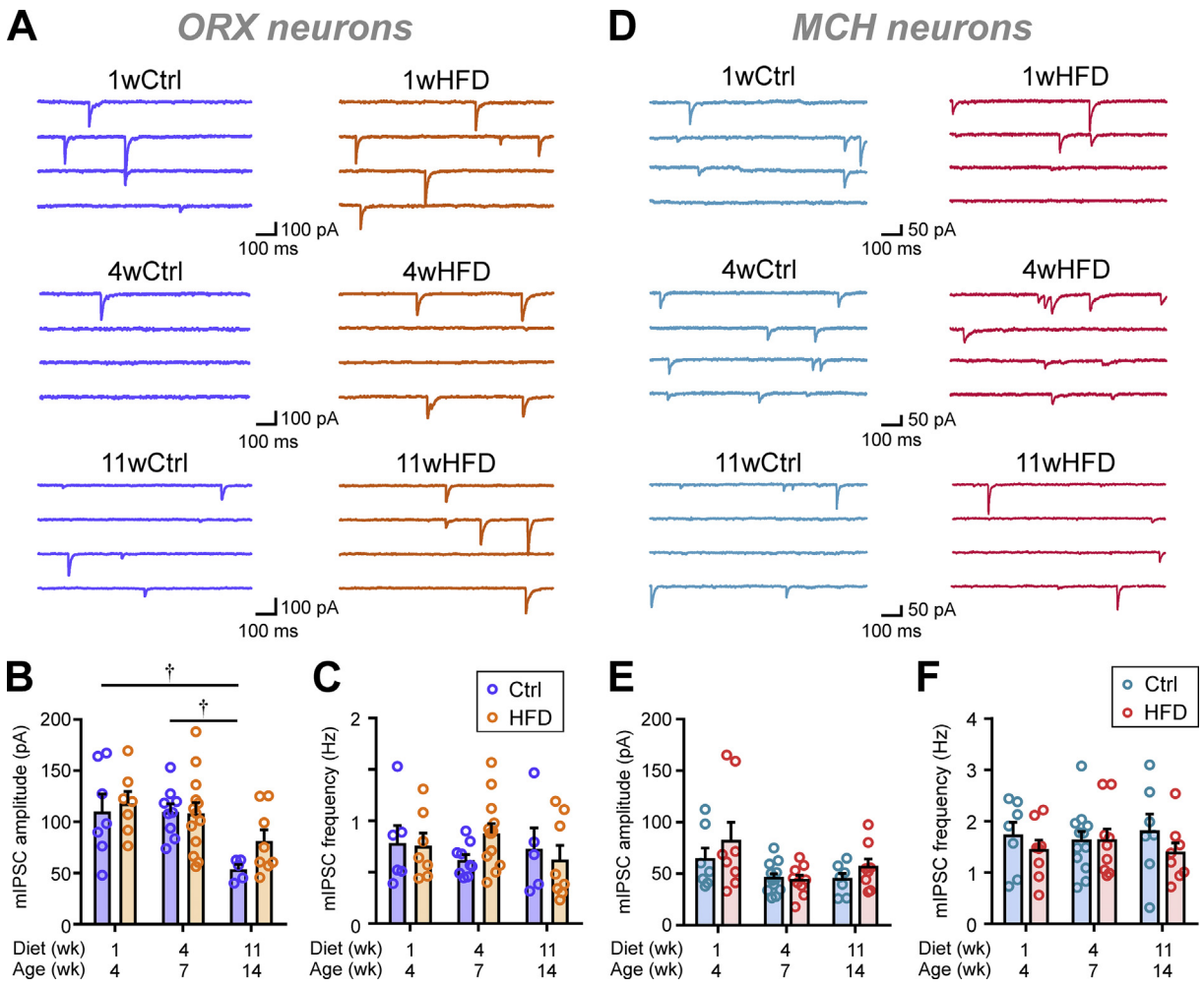

Figure 4: HFD does not affect spontaneous inhibitory transmission to ORX or MCH neurons. (A) Representative mIPSC traces of ORX neurons from Ctrl (left) or HFD (right) rats fed for 1, 4, and 11 weeks. (B–C) Summary graphs displaying no change in the mIPSC amplitude (B; two-way ANOVA, $p = 0.2618$) or frequency (C; two-way ANOVA, $p = 0.6794$) over the course of HFD feeding compared to the Ctrl group. mIPSC amplitude decreases with age among the Ctrl groups (one-way ANOVA, $p = 0.0007$), while mIPSC frequency does not change (one-way ANOVA, $p = 0.4699$). For (A–C): †$p < 0.05$ for age, Sidak's multiple comparison test. $n = 5–13$; $N = 3–5$. (D) Representative mIPSC traces of MCH neurons from Ctrl (left) or HFD (right) rats fed for 1, 4, and 11 weeks. (E–F) Summary graphs displaying a lack of HFD-induced change in the mIPSC amplitude (E; two-way ANOVA, $p = 0.2401$) and frequency (F; two-way ANOVA, $p = 0.2339$) throughout the feeding period. In Ctrl groups, there were also no age-dependent changes in mIPSC amplitude (one-way ANOVA, $p = 0.1879$) or frequency (one-way ANOVA, $p = 0.7971$). For (D–F): $n = 7–12$ cells; $N = 3–4$ rats.

However, HFD induced no significant changes in either mIPSC amplitude or frequency at any time point examined (Figure 4A–C).

Overall, our data indicate that ORX neurons experience acute increases in excitatory inputs during short-term HFD feeding (1–4 weeks) through multiple mechanisms. In contrast, inhibitory synaptic inputs undergo an age-dependent decrease in synaptic strength but are insensitive to HFD. The transient nature of HFD-induced changes suggests that ORX neurons functionally adapt to the diet after prolonged feeding.

3.2. Melanin concentration hormone neurons

In MCH neurons, HFD had no effect on the mEPSC amplitude (Figure 5A,C), peak of amplitude distribution (Figure 5B,D) or CV (Figure 5E) at any of the three time points assessed. As expected from a lack of change in mEPSC amplitude, a peak-scaled NSNA found no effect of HFD on either the estimated single channel current or number of channels (Figure 5F–G).

In contrast, the frequency of mEPSCs in the MCH neurons showed time-dependent effects of HFD. Specifically, 1 week of HFD induced a decrease in mEPSC frequency (Figure 6A–B). However, this reversed with time as the frequency became significantly higher compared to Ctrl after 4 weeks of HFD and continued to progressively increase with time (Figure 6A–B). These changes in mEPSC frequency occurred in the absence of any change in eEPSC amplitude or PPR (Figure 6C–E). This is consistent with the idea that HFD alters the number of active excitatory synaptic inputs to MCH neurons without affecting the presynaptic release probability.

To test this idea, a confocal immunofluorescence analysis was performed to assess the number of excitatory terminals in contact with MCH neurons. When rats were age-matched to adulthood, 1 week of HFD affected neither the amplitude nor the frequency of mEPSCs, while 4 weeks of HFD feeding increased mEPSC frequency (Figure 7A–B). Furthermore, the number of vGluT2-immunopositive excitatory terminals in apposition with MCH neuron somata significantly increased

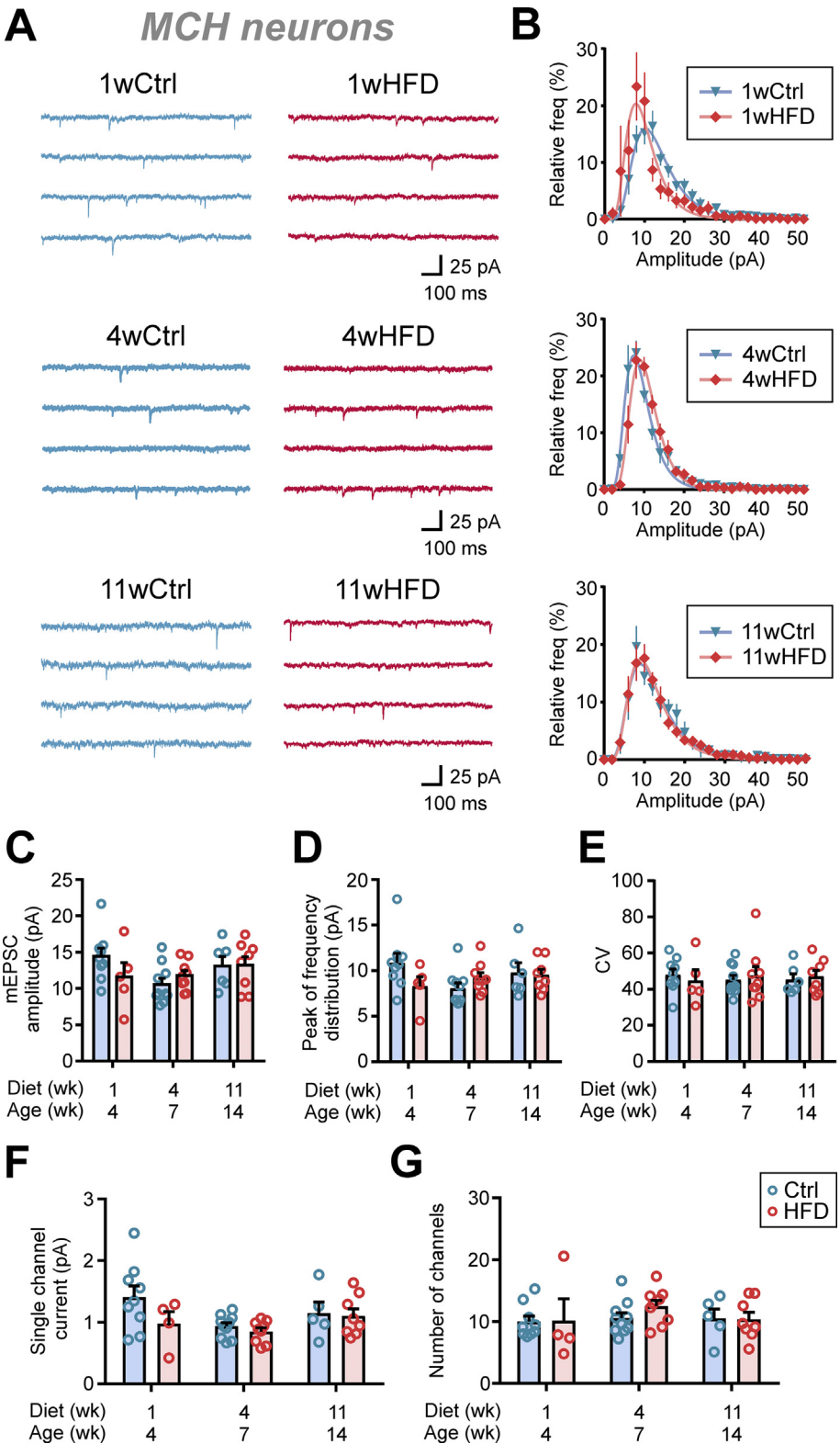

Figure 5: HFD has no effect on mEPSC amplitude in MCH neurons. (A) Representative mEPSC recordings from MCH neurons of Ctrl (left) and HFD (right) rats. (B) Relative frequency distribution of mEPSC amplitudes of MCH neurons. Plots represent averages of Ctrl or HFD groups. (C–E) Summary graphs showing that HFD has no effect on mEPSC amplitude (C; two-way ANOVA, $p = 0.5914$), the peak of relative frequency distribution shown in B (D; two-way ANOVA, $p = 0.4311$), and the coefficient of variation (CV) of mEPSC amplitude (E; two-way ANOVA, $p = 0.9115$). (F–G) Summary graphs displaying a lack of HFD-induced change in the estimated single channel current (F; two-way ANOVA, $p = 0.1005$) and the number of channels (G; two-way ANOVA, $p = 0.5553$). $n = 5–10$ cells; $N = 4–7$ rats.

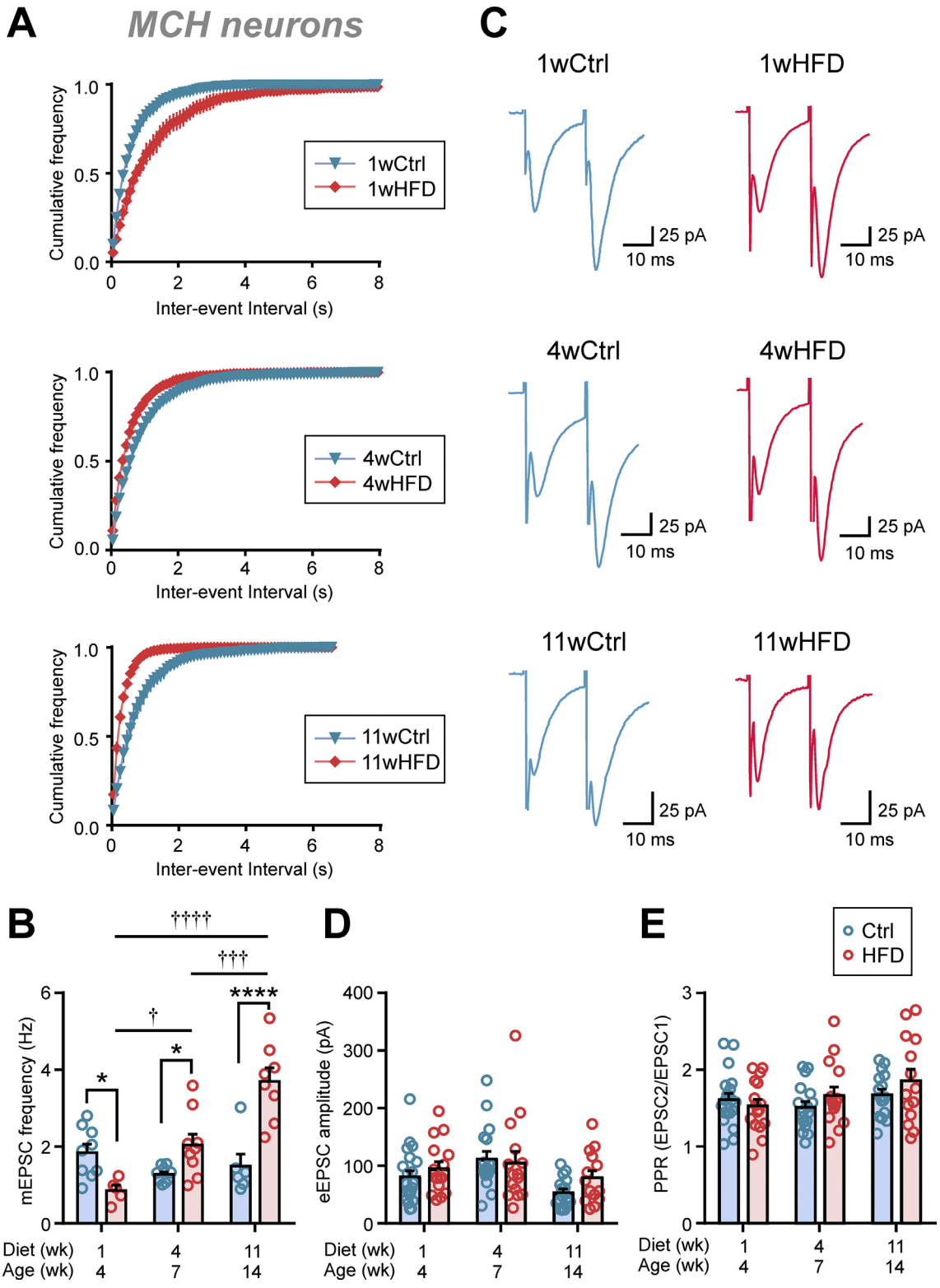

Figure 6: Chronic HFD persistently increases excitatory transmission to MCH neurons. (A) Average cumulative frequency distribution of mEPSC inter-event interval of MCH neurons. (B) HFD induces an initial decrease in mEPSC frequency, followed by a persistent increase relative to Ctrl (Two-way ANOVA, $p = 0.0034$). (C) Representative paired EPSCs from MCH neurons in Ctrl (left) and HFD (right) groups fed for the duration as indicated. (D) eEPSC amplitude is not altered by HFD (two-way ANOVA, $p = 0.2817$). (E) PPR is not altered by HFD (two-way ANOVA, $p = 0.2707$). *$p < 0.05$, ****$p < 0.0001$ for Ctrl vs HFD; †$p < 0.05$, †††$p < 0.005$, ††††$p < 0.0001$ for HFD duration, Sidak's multiple comparison test. $n = 5–21$ cells; $N = 4–16$ rats.

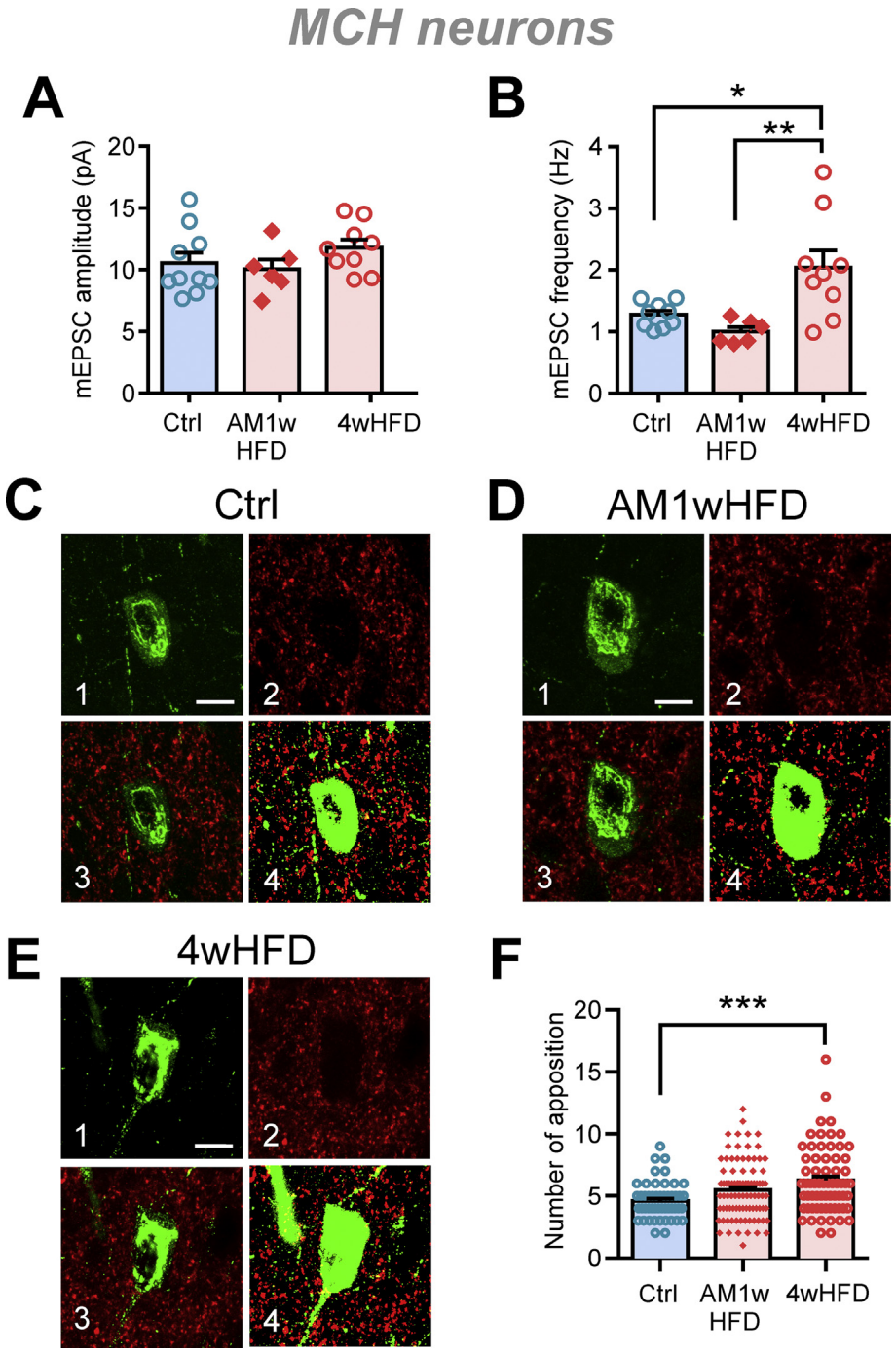

Figure 7: HFD induces a delayed increase in the number of excitatory synaptic contacts to MCH neurons. The feeding periods were staggered to age-match all groups (7 weeks old) at the time of assessment. AM1wHFD: age-matched 1-week HFD. (A) HFD feeding does not affect mEPSC amplitude in MCH neurons (one-way ANOVA, $p = 0.3180$). (B) HFD induces a delayed increase in mEPSC frequency (one-way ANOVA, $p = 0.0029$). For (A–B): $n = 6–9$ cells, $N = 4–6$ rats. $^{*}p < 0.05$, $^{**}p < 0.01$, Sidak's multiple comparison test. (C–E) Representative immunohistochemical images of the lateral hypothalamus of rats that were fed for the indicated time. The panels show an example of confocal immunofluorescence for MCH + neurons (green; C1, D1, and E1), vGluT2+ puncta (red; C2, D2, and E2), the merged confocal image containing both channels (C3, D3, and E3), and the merged binary image used for analysis (C4, D4, E4). Scale bar = 10 μm. (F) Four weeks of HFD feeding induced an increase in the number of vGluT2+ puncta apposed to the somata of MCH neurons (one-way ANOVA, $p = 0.0005$). For (C–F): $n = 52–90$ neurons from 2-4 slices per rat, $N = 3–4$ rats per diet condition. $^{***}p < 0.001$, Sidak's multiple comparison test.

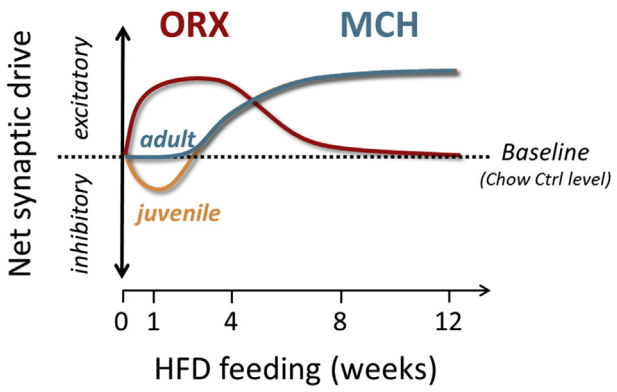

Figure 8: Net change in synaptic properties of ORX and MCH neurons over the course of HFD feeding. A schematic summarizing the time course of synaptic changes in ORX and MCH neurons due to HFD. In ORX neurons, excitatory synaptic transmission increases during the acute phase (from 1 day to 4 weeks). All of the excitatory changes return to chow Ctrl levels (baseline) by week 11 of HFD. In contrast, HFD does not influence inhibitory synaptic transmission. Thus, the net change in synaptic drive or the balance between excitatory and inhibitory synaptic inputs to ORX neurons is excitatory in the early phase of HFD, which normalizes with prolonged feeding. In MCH neurons, excitatory synaptic transmission decreases after the first week of HFD. Note that this inhibitory effect is specific to adolescence and is not seen in adulthood. As the HFD exposure persists, the excitatory synaptic drive starts to increase by week 4 and continues to increase with prolonged feeding. In contrast, HFD has no effect on inhibitory synaptic transmission to MCH neurons. Thus, the net synaptic drive follows the changes in excitatory transmission.

after 4 weeks but not after 1 week of HFD feeding (Figure 7C—F). These results together suggest that in adulthood, prolonged HFD induces a delayed increase in the number of excitatory synaptic contacts to MCH neurons.

In contrast to the dynamic changes in excitatory synaptic transmission, mIPSC amplitude and frequency in MCH neurons were unaffected by HFD or age (Figure 4D—F). These data suggest that the basal activity of inhibitory synaptic inputs to MCH neurons is insensitive to HFD.

Together, these results indicate that the net effect of HFD on MCH neurons changes over time. Initially (1 week), excitatory inputs decrease (in adolescence) or do not change (adulthood). The age dependence of this inhibitory effect may be due to underlying developmental changes in basal synaptic transmission during adolescence [30]. With prolonged HFD exposure (4—11 weeks), excitatory inputs increase while inhibitory inputs do not change, suggesting a net increase in the excitatory drive. Therefore, HFD induces time-dependent alterations in the balance between excitatory and inhibitory synaptic inputs to MCH neurons.

3.3. Synaptic effects of HFD in mice

To determine whether our findings in rats are also applicable to other species, we assessed the long-term effect of HFD (13—16 weeks) in mice. As expected, HFD induced an increase in body weight and caloric intake compared to chow Ctrl (Figures S4A—C). We found that ORX neurons from Ctrl or HFD mice showed no significant differences in the frequency or amplitude of mEPSCs and mIPSCs (Figures S4D—E). In contrast, mEPSC frequency in MCH neurons significantly increased without any change in mEPSC amplitude (Figure S4F). However, there was no significant change in mIPSCs in MCH neurons (Figure S4G). These were similar to the effects observed in rats, indicating that the synaptic effects of long-term HFD were consistent between species.

4. DISCUSSION

The present study demonstrates that ORX and MCH neurons undergo synaptic plasticity during HFD in a cell-type specific, feeding duration-dependent manner (Figure 8). On one hand, ORX neurons display excitatory changes early in the HFD feeding period, which normalizes as the diet becomes chronic. On the other hand, MCH neurons initially show reduced excitatory drive, followed by a delayed and persistent increase in excitatory transmission that precedes the onset of significant weight gain. The initial decrease is age dependent and is only seen during adolescence. These differential effects of HFD may underlie the complementary and partially antagonistic roles of these cells in energy balance. The mechanism by which HFD induces synaptic remodeling remains unclear; however, metabolic and hormonal changes associated with HFD may be involved. For example, leptin, insulin, endocannabinoids and brain-derived neurotrophic factor have been shown to mediate HFD-induced synaptic remodeling in various brain regions [2,34,35]. ORX and MCH neurons directly receive widely distributed afferents from overlapping and discrete brain areas involved in energy balance and reward and sleep/wake control, including many nuclei in the hypothalamus, other subcortical and cortical areas, and the midbrain [7]. Some of these direct inputs are indeed glutamatergic [36—39]. It remains unknown whether all of these or selective pathways are sensitive to HFD and whether the same synapses undergo dynamic plasticity over the course of HFD or different sets of synapses show plasticity at different time points.

ORX neurons display an acute increase in excitatory transmission as early as 1 day of HFD, which appears to be due to an increase in the single channel current mediated by postsynaptic AMPA receptors [40]. Glutamatergic synaptic activity has been shown to underlie basal excitability of ORX neurons [41]. Thus, increased excitatory drive along with known upregulation of ORX mRNA by short-term HFD exposure [42] will likely lead to an increased release of ORX peptide. Released ORX may stimulate downstream targets in the reward system such as the ventral tegmental area [43], which is also known to undergo rapid synaptic plasticity in response to palatable food consumption [44]. In this light, these plastic changes may influence the rewarding value of palatable diets and reinforce further consumption by promoting motivation and food seeking. In fact, non-food rewards, such as cocaine, have been demonstrated to induce synaptic alterations in ORX neurons [45,46], suggesting that these cells respond with synaptic plasticity to rewarding stimuli in general.

By week 4, the change in mEPSC amplitude normalizes, while mEPSC frequency increases in ORX neurons. This does not accompany any change in PPR, which could be explained by an increase in active excitatory synapses rather than release probability. However, this was not supported by a confocal analysis that found no change in the number of excitatory terminals in apposition with ORX neurons. The possibility of synaptic remodeling at the dendrites cannot be excluded as our confocal analysis was limited to somatic contacts. However, a similar confocal analysis successfully detected changes in the number of vGluT2-expressing terminals making somatic contact with ORX neurons in obese mice [34]. Alternatively, structural components of synapses can exist but be functionally quiescent [47], which could dissociate electrophysiological and immunohistochemical results. Furthermore, the discrepancy may be partially explained if only a subpopulation of ORX neurons responds to HFD. For example, ORX neurons have been subdivided into two groups based on their electrophysiological properties [48], which display differential responses to glucose [49] and sleep deprivation [50]. As these subpopulations

cannot be segregated histochemically, changes in one subpopulation may be masked by a lack of change in other ORX subtypes.

As feeding becomes chronic, HFD-induced effects on ORX neurons reverse to Ctrl levels. This reversal of electrophysiological changes combined with reported decreases in ORX mRNA expression with long periods of high-fat feeding (>1 month) [51,52] suggest that the output from ORX neurons may be reduced during chronic HFD conditions. This may contribute to a dampening of reward function by dietary fat [53] or a permissive condition for DIO through diminished energy expenditure [54].

Of note, previous studies have shown that excitatory synapses and intrinsic properties of ORX neurons gradually develop postnatally and reach the adult level by 3 weeks of age (before the adolescence period) in rodents [30,55]. In the present study, the excitatory effect of short-term HFD (1 week) was consistently observed after this developmental period, namely at 4 and 7 weeks of age, further confirming the functional maturation of ORX neurons. However, we saw a significant decrease in mIPSC amplitude in the chow Ctrl group after 7 weeks of age, indicating that some aspects of functional maturation of ORX neurons continue past adolescence.

Unlike the dynamic changes in excitatory transmission, HFD did not induce any change in inhibitory transmission in ORX neurons throughout the feeding period. This is in contrast to a previous report that showed an increase in mIPSC amplitude in ORX neurons after 16 weeks of HFD feeding [34]. Possible explanations for this discrepancy could be the difference in species (mice vs rats), diets, and/or the feeding duration. Alternatively, as our data from rat ORX neurons trend toward an increase in mIPSC amplitude after 11 weeks of HFD, it may become more pronounced if the diet continues, which would be consistent with the previous report.

In contrast to ORX neurons, our results suggest that MCH neurons respond to short-term HFD with a decrease in excitatory transmission, which may be a homeostatic compensatory response to the diet. However, this inhibitory effect is specific to the adolescence period as it was not observed in adult rats. This is similar to a previous report demonstrating that HFD induces certain changes in the hippocampus when commenced during the juvenile period (3 weeks old) but not during adulthood [56]. These studies suggest that the effects of HFD on the brain of developing and mature animals are not identical.

The acute phase is followed by a persistent increase in the frequency of mEPSCs in the absence of a significant change in mIPSCs, which can be expected to increase the excitability of these neurons. This was accompanied by a significant increase in the number of excitatory terminals apposing MCH neurons, suggesting that synaptic remodeling occurred. Importantly, these changes occur before (4 weeks of HFD) the onset of excess weight gain (around 5 weeks of HFD) and its magnitude progressively intensifies with longer HFD feeding, suggesting that the observed effects are unlikely to be a result of obesity. Given the role of MCH in positive energy balance, the timing of the onset and continuance of elevated excitatory drive to MCH neurons may contribute to the development and maintenance of DIO.

Previous studies have shown that ORX and MCH neurons undergo various forms of synaptic plasticity during obese states or HFD feeding. For example, DIO or leptin deficiency changes the expression of cannabinoid receptors on excitatory and inhibitory synaptic terminals, resulting in altered endocannabinoid-dependent control of ORX neurons [34,57]. Leptin-deficient mice also display altered endocannabinoid-mediated synaptic inhibition in perifornical neurons, about half of which were identified as MCH neurons [58]. Furthermore, HFD impairs the thermosensitivity of ORX neurons [31] and leptin-induced inhibition of excitatory transmission to MCH and ORX neurons [44]. Time-dependent plasticity has also been observed, where excitatory synapses to ORX neurons are primed for long-term depression after 1 week of HFD feeding, but not after 4 weeks [59]. Therefore, HFD can also induce other plastic and metaplastic changes that could collectively shape the synaptic inputs that regulate the excitability of these neurons.

5. CONCLUSION

The present study is the first to investigate time-dependent HFD-induced changes in spontaneous synaptic transmission in lateral hypothalamic cell populations. Over the course of HFD feeding, multiple forms of synaptic plasticity were found depending on the cell type and length of feeding. As energy balance is coordinated by many neuronal populations, synaptic plasticity in ORX and MCH neurons are unlikely to be the sole determinant of the response to HFD but may nevertheless impact the overall activity and output of the feeding circuitry. As summarized in Figure 8, in the short term, ORX neurons receive an increased excitatory drive and may mediate the rewarding aspect of HFD consumption [19]. In the long term, reversal of the excitatory effects on ORX neurons may provide a permissive condition for weight gain [25], while a delayed increase in excitatory inputs to MCH neurons could contribute to the development and maintenance of DIO [28,29]. This complex, time-dependent synaptic plasticity suggests that the HFD effects on feeding-related neurons are dynamic and not necessarily stable. This highlights the importance of considering feeding duration when comparing studies and choosing the appropriate timing for investigation and weight loss interventions.

FUNDING

This study was funded by the Canadian Institutes of Health Research (CIHR PJT-153173) to MH. VL was a recipient of the CIHR/RDC Doctoral Research Award. LZF was a recipient of the Heart and Stroke Foundation Graduate Scholarship and the CIHR Doctoral Research Award.

ACKNOWLEDGMENTS

We gratefully acknowledge Josué Lily Vidal, Nick Newhook, and Christie Costello for their technical assistance. We also thank Memorial University's Medical Laboratories-Confocal Microscopy Unit for their technical support.

CONFLICT OF INTEREST

None declared.

APPENDIX A. SUPPLEMENTARY DATA

Supplementary data to this article can be found online at https://doi.org/10.1016/j.molmet.2020.100977.

REFERENCES

[1] Horvath, T.L., Sarman, B., García-Cáceres, C., Enriori, P.J., Sotonyi, P., Shanabrough, M., et al., 2010. Synaptic input organization of the melanocortin system predicts diet-induced hypothalamic reactive gliosis and obesity. Proceedings of the National Academy of Sciences of the U S A 107:14875–14880.

[2] Pinto, S., Roseberry, A.G., Liu, H., Diano, S., Shanabrough, M., Cai, X., et al., 2004. Rapid rewiring of arcuate nucleus feeding circuits by leptin. Science 304:110–115.

[3] Rada, P., Avena, N.M., Barson, J.R., Hoebel, B.G., Leibowitz, S.F., 2012. A high-fat meal, or intraperitoneal administration of a fat emulsion increases extracellular dopamine in the nucleus accumbens. Brain Sciences 2:242—253.
[4] Schwartz, M.W., Woods, S.C., Porte Jr., D., Seeley, R.J., Baskin, D.G., 2000. Central nervous system control of food intake. Nature 404:661—671.
[5] Kenny, P.J., 2011. Common cellular and molecular mechanisms in obesity and drug addiction. Nature Reviews Neuroscience 12:638—651.
[6] Barson, J.R., Morganstern, I., Leibowitz, S.F., 2013. Complementary roles of orexin and melanin-concentrating hormone in feeding behavior. The Internet Journal of Endocrinology, 1—10.
[7] González, J.A., Iordanidou, P., Strom, M., Adamantidis, A., Burdakov, D., 2016. Awake dynamics and brain-wide direct inputs of hypothalamic MCH and orexin networks. Nature Communications 7:1—9.
[8] González, J.A., Jensen, L.T., Fugger, L., Burdakov, D., 2012. Convergent inputs from electrically and topographically distinct orexin cells to locus coeruleus and ventral tegmental area. European Journal of Neuroscience 35: 1426—1432.
[9] Bittencourt, J.C., 2011. Anatomical organization of the melanin-concentrating hormone peptide family in the mammalian brain. General and Comparative Endocrinology 172:185—197.
[10] Muroya, S., Funahashi, H., Yamanaka, A., Kohno, D., Uramura, K., Nambu, T., et al., 2004. Orexins (hypocretins) directly interact with neuropeptide Y, POMC and glucose-responsive neurons to regulate Ca^{2+} signaling in a reciprocal manner to leptin: orexigenic neuronal pathways in the mediobasal hypothalamus. European Journal of Neuroscience 19:1524—1534.
[11] Sakurai, T., Amemiya, A., Ishii, M., Matsuzaki, I., Chemelli, R.M., Tanaka, H., et al., 1998. Orexins and orexin receptors: a family of hypothalamic neuropeptides and G Protein-Coupled receptors that regulate feeding behavior. Cell 92:573—585.
[12] Qu, D., Ludwig, D.S., Gammeltoftt, S., Piper, M., Pelleymounter, M.A., Cullen, M.J., et al., 1996. A role for melanin-concentrating hormone in the central regulation of feeing behaviour. Nature 380:243—247.
[13] Haynes, A.C., Jackson, B., Overend, P., Buckingham, R.E., Wilson, S., Tadayyon, M., et al., 1999. Effects of single and chronic intracerebroventricular administration of the orexins on feeding in the rat. Peptides 20:1099—1105.
[14] Della-Zuana, O., Presse, F., Ortola, C., Duhault, J., Nahon, J.L., Levens, N., 2002. Acute and chronic administration of melanin-concentrating hormone enhances food intake and body weight in Wistar and Sprague—Dawley rats. International Journal of Obesity 26:1289—1295.
[15] Gomori, A., Ishihara, A., Ito, M., Matsushita, H., Yumoto, M., Ito, M., et al., 2002. Chronic intracerebroventricular infusion of MCH causes obesity in mice. American Journal of Physiology. Endocrinology and Metabolism 264:583—588.
[16] Chang, G.-Q., Karatayev, O., Davydova, Z., Leibowitz, S.F., 2004. Circulating triglycerides impact on orexigenic peptides and neuronal activity in hypothalamus. Endocrinology 145:3904—3912.
[17] Petrovich, G.D., Hobin, M.P., Reppucci, C.J., 2012. Selective Fos induction in hypothalamic orexin/hypocretin, but not melanin-concentrating hormone neurons, by a learned food-cue that stimulates feeding in sated rats. Neuroscience 224:70—80.
[18] Choi, D.L., Davis, J.F., Fitzgerald, M.E., Benoit, S.C., 2010. The role of orexin-A in food motivation, reward-based feeding behavior and food-induced neuronal activation in rats. Neuroscience 167:11—20.
[19] Harris, G.C., Wimmer, M., Aston-Jones, G., 2005. A role for lateral hypothalamic orexin neurons in reward seeking. Nature 437:556—559.
[20] Moorman, D.E., James, M.H., Kilroy, E.A., Aston-Jones, G., 2016. Orexin/hypocretin neuron activation is correlated with alcohol seeking and preference in a topographically specific manner. European Journal of Neuroscience 43: 710—720.
[21] Plaza-Zabala, A., Maldonado, R., Berrendero, F., 2012. The hypocretin/orexin system: implications for drug reward and relapse. Molecular Neurobiology 45: 424—439.
[22] Hara, J., Beuckmann, C.T., Nambu, T., Willie, J.T., Chemelli, R.M., Sinton, C.M., et al., 2001. Genetic ablation of orexin neurons in mice results in narcolepsy, hypophagia, and obesity. Neuron 30:345—354.
[23] Inutsuka, A., Inui, A., Tabuchi, S., Tsunematsu, T., Lazarus, M., Yamanaka, A., 2014. Concurrent and robust regulation of feeding behaviors and metabolism by orexin neurons. Neuropharmacology 85:451—460.
[24] Shirasaka, T., Nakazato, M., Shigeru, M., Takasaki, M., Kannan, H., 1999. Sympathetic and cardiovascular actions of orexins in conscious rats. American Journal of Physiology 277:R1780—R1785.
[25] Zink, A.N., Bunney, P.E., Holm, A.A., Billington, C.J., Kotz, C.M., 2018. Neuromodulation of orexin neurons reduces diet-induced adiposity. International Journal of Obesity 42:737—745.
[26] Domingos, A.I., Sordillo, A., Dietrich, M.O., Liu, Z.W., Tellez, L.A., Vaynshteyn, J., et al., 2013. Hypothalamic melanin concentrating hormone neurons communicate the nutrient value of sugar. Elife 2:1—15.
[27] Clegg, D.J., Air, E.L., Woods, S.C., Seeley, R.J., 2002. Eating elicitied by orexin-a, but not melanin-concentrating hormone, is opioid mediated. Endocrinology 143:2995—3000.
[28] Alon, T., Friedman, J.M., 2006. Late-onset leanness in mice with targeted ablation of melanin concentrating hormone neurons. Journal of Neuroscience 26:389—397.
[29] Mul, J.D., Yi, C.-X., van den Berg, S.A., Ruiter, M., Toonen, P.W., van der Elst, M.C., et al., 2009. Pmch expression during early development is critical for normal energy homeostasis. American Journal of Physiology. Endocrinology and Metabolism 298:E477—E488.
[30] Linehan, V., Hirasawa, M., 2018. Electrophysiological properties of melanin-concentrating hormone and orexin neurons in adolescent rats. Frontiers in Cellular Neuroscience 12:1—10.
[31] Belanger-Willoughby, N., Linehan, V., Hirasawa, M., 2016. Thermosensing mechanisms and their impairment by high-fat diet in orexin neurons. Neuroscience 324:82—91.
[32] Linehan, V., Trask, R.B., Briggs, C., Rowe, T.M., Hirasawa, M., 2015. Concentration-dependent activation of dopamine receptors differentially modulates GABA release onto orexin neurons. European Journal of Neuroscience 42: 1976—1983.
[33] Benke, T.A., Lüthi, A., Isaac, J.T.R., Collingridge, G.L., 1998. Modulation of AMPA receptor unitary conductance by synpatic activity. Nature 393:793—797.
[34] Cristino, L., Busetto, G., Imperatore, R., Ferrandino, I., Palomba, L., Silvestri, C., et al., 2013. Obesity-driven synaptic remodeling affects endocannabinoid control of orexinergic neurons. Proceedings of the National Academy of Sciences of the U S A 110:E2229—E2238.
[35] Stranahan, A.M., Norman, E.D., Lee, K., Cutler, R.G., Telljohann, R.S., Egan, J.M., et al., 2009. Diet-induced insulin resistance impairs hippocampal synaptic plasticity and cognition in middle-aged rats. Hippocampus 18:1085—1088.
[36] Henny, P., Jones, B.E., 2006. Innervation of orexin/hyopcretin neurons by GABAergic, glutamatergic or cholinergic basal forebrain terminals evidenced by immunostaining for presynaptic vesicular transporter and postsynaptic scaffolding proteins. The Journal of Comparative Neurology 499:645—661.
[37] Niu, J.G., Yokota, S., Tsumori, T., Qin, Y., Yasui, Y., 2010. Glutamatergic lateral parabrachial neurons innervate orexin-containing hypothalamic neurons in the rat. Brain Research 1358:110—122.
[38] Niu, J.G., Yokota, S., Tsumori, T., Oka, T., Yasui, Y., 2012. Projections from the anterior basomedial and anterior cortical amygdaloid nuceli to melanin-concentrating hormone-containing neurons in the lateral hypothalamus of the rat. Brain Research 14779:31—43.

[39] Bochorishvili, G., Nguyen, T., Coates, M.B., Viar, K.E., Stornetta, R.L., Guyenet, P.G., 2014. The orexinergic neurons receive synaptic input from C1 cells in rats. The Journal of Comparative Neurology 522:3834—3846.

[40] Alberto, C.O., Hirasawa, M., 2010. AMPA receptor-mediated miniature EPSCs have heterogeneous time courses in orexin neurons. Biochemical and Biophysical Research Communications 400:707—712.

[41] Li, Y., Gao, X.B., Sakurai, T., van den Pol, A.N., 2002. Hypocretin/Orexin excites hypocretin neurons via a local glutamate neuron — a potential mechanism for orchestrating the hypothalamic arousal system. Neuron 36: 1169—1181.

[42] Wortley, K.E., Chang, G.-Q., Davydova, Z., Leibowitz, S.F., 2003. Peptides that regulate food intake orexin gene expression is increased during states of hypertriglyceridemia. Am J Physiol Integr Comp Physiol 284:1454—1465.

[43] Terrill, S.J., Hyde, K.M., Kay, K.E., Greene, H.E., Maske, C.B., Knierim, A.E., et al., 2016. Ventral tegmental area orexin 1 receptors promote palatable food intake and oppose postingestive negative feedback. Am J Physiol Integr Comp Physiol 311:592—599.

[44] Liu, J.-J., Bello, N.T., Pang, Z.P., 2017. Presynaptic regulation of leptin in a defined lateral hypothalamus — ventral tegmental area neurocircuitry depends on energy state. Journal of Neuroscience 37:11854—11866.

[45] Yeoh, J.W., James, M.H., Jobling, P., Bains, J.S., Graham, B.A., Dayas, C.V., 2012. Cocaine potentiates excitatory drive in the perifornical/lateral hypothalamus. Journal of Physiology 590:3677—3689.

[46] Rao, Y., Mineur, Y.S., Gan, G., 2013. Repeated in vivo exposure of cocaine induces long-lasting synaptic plasticity in hypocretin/orexin-producing neurons in the lateral hypothalamus in mice. Journal of Physiology 591:1951—1966.

[47] Chang, C.Y., Jiang, X., Moulder, K.L., Mennerick, S., 2010. Rapid activation of dormant presynaptic terminals by phorbol esters. Journal of Neuroscience 30: 10048—10060.

[48] Schone, C., Venner, A., Knowles, D., Karnani, M.M., Burdakov, D., 2011. Dichotomous cellular properties of mouse orexin/hypocretin neurons. Journal of Physiology 589:2767—2779.

[49] Williams, R.H., Alexopoulos, H., Jensen, L.T., Fugger, L., Burdakov, D., 2008. Adaptive sugar sensors in the hypothalamic feeding circuits. Proceedings of the National Academy of Sciences of the United States of America 105: 11975—11980.

[50] Briggs, C., Bowes, S.B., Semba, K., Hirasawa, M., 2019. Sleep deprivation-induced pre- and postsynaptic modulation of orexin neurons. Neuropharmacology 154:50—60.

[51] Novak, C.M., Escande, C., Burghardt, P.R., Zhang, M., Barbosa, M.T., Chini, E.N., et al., 2010. Spontaneous activity, economy of activity, and resistance to diet-induced obesity in rats bred for high intrinsic aerobic capacity. Hormones and Behavior 58:355—367.

[52] Tanno, S., Terao, A., Okamatsu-Ogura, Y., Kimura, K., 2013. Hypothalamic prepro-orexin mRNA level is inversely correlated to the non-rapid eye movement sleep level in high-fat diet-induced obese mice. Obesity Research & Clinical Practice 7:e251—e257.

[53] Hryhorczuk, C., Florea, M., Rodaros, D., Poirier, I., Daneault, C., Des Rosiers, C., et al., 2016. Dampened mesolimbic dopamine function and signaling by saturated but not monounsaturated dietary lipids. Neuropsychopharmacology 41:811—821.

[54] Hagan, J.J., Leslie, R.A., Patel, S., Evans, M.L., Wattam, T.A., Holmes, S., Benham, C.D., et al., 1999. Orexin A activates locus coeruleus cell firing and increases arousal in the rat. Proceedings of the National Academy of Sciences of the U S A 96:10911—10916.

[55] Ogawa, Y., Kanda, T., Vogt, K., Yanagisawa, M., 2017. Anatomical and electrophysiological development of the hypothalamic orexin neurons from embryos to neonates. The Journal of Comparative Neurology 525:3809—3820.

[56] Boitard, C., Etchamendy, N., Sauvant, J., Aubert, A., Tronel, S., Marighetto, A., et al., 2012. Juvenile, but not adult exposure to high-fat diet impairs relational memory and hippocampal neurogenesis in mice. Hippocampus 22:2095—2100.

[57] Becker, T.M., Favero, M., Di Marzo, V., Cristino, L., Busetto, G., 2017. Endocannabinoid-dependent disinhibition of orexinergic neurons: electrophysiological evidence in leptin-knockout obese mice. Mol Metab 6:594—601.

[58] Jo, Y.-H., Chen, Y.-J.J., Chua Jr., S.C., Talmage, D.A., Role, L.W., 2005. Integration of endocannabinoid and leptin signaling in an appetite-related neural circuit. Neuron 48:1055—1066.

[59] Linehan, V., Fang, L.Z., Hirasawa, M., 2018. Short-term high-fat diet primes excitatory synapses for long-term depression in orexin neurons. Journal of Physiology 2:305—316.

